

Article

# Research on Machining Error Analysis and Traceability Method of Globoidal Indexing Cam Profile

Shuwen Sun <sup>\*</sup>, Yunfei Qiao, Zhentao Gao and Chao Huang

Faculty of Materials and Manufacturing, Beijing University of Technology, Beijing 100124, China; qiaoyf@emails.bjut.edu.cn (Y.Q.); gzt365937954@emails.bjut.edu.cn (Z.G.); hc13672039682@163.com (C.H.)  
\* Correspondence: sshwen@bjut.edu.cn

**Abstract:** The profile of the globoidal indexing cam is a spatially undevelopable surface. It needs a special computer numerical control (CNC) machine tool to finish batch production, and its machining quality will be affected by the motion error of each part of the machine tool and the clamped positioning error of the workpiece. Firstly, the mathematical model of the error of the machine tool for machining the globoidal cam surface is derived, and the influence of the error of the machine tool for machining the globoidal cam surface is given. Secondly, an error tracking method for globoidal cam profile machining error based on error sensitivity coefficient grouping is proposed, which improves the data processing speed and the accuracy of the tracking results. Finally, the error analysis and traceability method of the globoidal cam is verified by experiments, and the error traceability results are fed back to the processing link. The machining quality of globoidal cam is improved by the error compensation, which provides the key technology for the integration of the design, manufacture, and measurement of the globoidal cam.

**Keywords:** error sensitivity; error traceability; globoidal indexing cam; machining error model; multi-body theory



**Citation:** Sun, S.; Qiao, Y.; Gao, Z.; Huang, C. Research on Machining Error Analysis and Traceability Method of Globoidal Indexing Cam Profile. *Machines* **2022**, *10*, 219. <https://doi.org/10.3390/machines10030219>

Academic Editor: Angelos P. Markopoulos

Received: 18 February 2022

Accepted: 17 March 2022

Published: 21 March 2022

**Publisher's Note:** MDPI stays neutral with regard to jurisdictional claims in published maps and institutional affiliations.



**Copyright:** © 2022 by the authors. Licensee MDPI, Basel, Switzerland. This article is an open access article distributed under the terms and conditions of the Creative Commons Attribution (CC BY) license (<https://creativecommons.org/licenses/by/4.0/>).

## 1. Introduction

The globoidal cam indexing mechanism has the advantages of a compact structure, high indexing precision, strong bearing capacity, and good high-speed performance. Consequently, the globoidal cam mechanism plays a pivotal role in mechanical transmission, so it has been widely used in the automatic tool changer (ATC) of computer numerical control (CNC), tobacco machinery, packaging machinery, aerospace, automatic machine tools, and in other fields [1,2]. The globoidal indexing cam is a key component in ATC. Because ATC requires a high precision globoidal cam profile, the manufacture and tolerance detection of a high-grade globoidal cam has been a difficult problem for domestic enterprises [3,4]. The globoidal cam profile is a non-developable surface in space, which is difficult to process. The profile error of the globoidal cam will directly reduce the output accuracy of the ATC and seriously affect the grasping and positioning accuracy of the manipulator. Five-axis CNC machine tools are generally used for the machining of globoidal cams, so the processing strategy of five-axis CNC machine tools is extremely important. By optimizing the machining strategy, the machining quality of the workpiece can be improved. Amaia Calleja studied the optimal machining strategy for blade turning and milling and tested different strategies and inclination angles to obtain the best blade machining parameters and toolpath strategies [5]. Therefore, in the manufacturing process, the CNC machine tool should be analyzed in detail to ensure the machining accuracy of the globoidal cam. It is of great practical significance to study the machining error and detection of globoidal cam [6,7].

There are several scholars who have studied the machining error of globoidal cams. H.Y. Cheng analyzed the error transfer of globoidal indexing cam mechanism systematically and established the error transfer equation. At the same time, he analyzed the

sensitivity made by output precision to each error and established the sensitivity equation [8]. An improved optimal deviation method to study the more reasonable allocation of globoidal cam mechanism tolerance was proposed by Yang Shiping [9]. Yin Mingfu researched the influence caused by the center distance error of a globoidal indexing cam machine tool on cam profile error and gave the changing trend of error [10]. Ji Shuting researched the influence caused by the center distance error of the globoidal indexing cam special machining on the cam profile machining error and drew the influence coefficient curve. She revealed the result that the center distance error leads to the error of globoidal indexing cam profile [11,12]. Based on the above research, the influence caused by two rotation shaft errors, three vertical errors, and three linear displacement errors of globoidal indexing cam special machining on the machining error of the globoidal indexing cam profile has been analyzed [13]. Tang Lin measured in the three-coordinate measuring machine (CMM) and introduced the concept of profile tolerance and helix tolerance [14]. P.D. Lin and J.F. Hsieh researched the conversion between the measurement coordinates and the theoretical position, to determine the measuring benchmark [15]. Song Lijuan proposed reversely obtaining the manufacturing tolerance by measuring results [16], but she did not research the specific contents. Lin Xiaojun proposed a method to compensate the radius by reconstructing the equidistant surface [17].

However, the measuring speed of the current CMM method is slow and complex. It cannot meet the measurement requirements of globoidal cams in the production line, and it is difficult to fundamentally solve the problem of radius compensation. To solve the incongruity error of the normal vector of globoidal cams in non-equal-diameter machining, Hu Dongfang improved the tool axis vector by using the space linear regression algorithm and the ruled surface generation principle and realized the optimization of the tool path [18,19]. In addition, an adaptive compensation method for tool position error was also proposed, which greatly improves the machining accuracy of the globoidal cam in unequal diameter machining. Hammoudi Abderazek applied seven meta-heuristic optimization algorithms to design the disk cam mechanism, formulated three objective design problems, and studied the influence of the selection of the motion law of the follower on the optimal design of the mechanism [20]. Nguyen proposed a general framework for the kinematic design of cam mechanisms based on non-uniform rational B-splines (NURBS) to reduce inertial forces and vibration trends in cam dynamics of high-speed cam systems [21]. Sateesh represented the displacement function with NURBS based on standard displacement curves of the follower [22]. Xia Bizhong realized the design of the cam profile by combining the sixth-order classical spline and the general polynomial spline. After experimental verification, the improved cam profile demonstrated better performance [23]. In 2018, our team published the conference paper “Analysis and Detection Method for Machining Error of Globoidal Indexing Cam Profile” [24] and proposed a globoidal cam error detection method based on equidistant contour. Since then, the research has continued, and the globoidal cam design–machining–measuring integrated technology has been formed. In order to ensure the integrity of the research content, the content of the machining error analysis of the machine tool in the 2018 conference paper is included in this paper.

In this paper, we propose a general method of globoidal indexing cam profile machining error analysis and traceability. According to the working principle of the globoidal cam machine, the mathematical model of the globoidal cam profile error is established by using the multi-body system theory. An error evaluation and traceability method based on the equidistant model characteristic line of the globoidal cam is proposed. This method can be used for error compensation in the machining process of the globoidal cam to improve the machining accuracy. The integrated technology of globoidal cam design, manufacture, and measurement is shown in Figure 1.

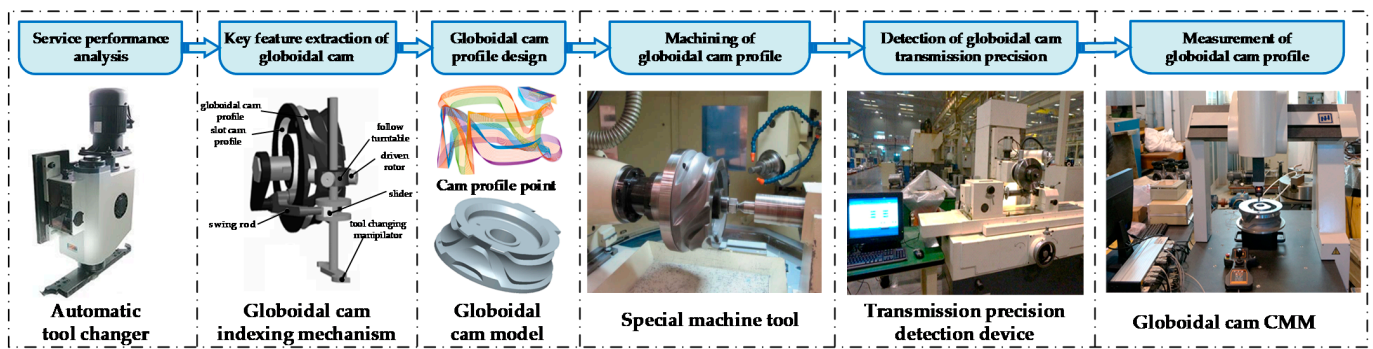


Figure 1. Schematic of globoidal cam design, manufacture and measurement integration.

The remainder of the paper is organized as follows. An analysis model of globoidal cam machining error based on multi-body system theory is established in Section 2. The error evaluation and traceability of globoidal cam machining errors are provided out in Section 3. Finally, the integration of design–machining–measuring–evaluation and traceability of the globoidal cam was realized in the factory, and the experimental research on the profile error detection globoidal cam is introduced in detail in Section 4, while conclusions are drawn in Section 5.

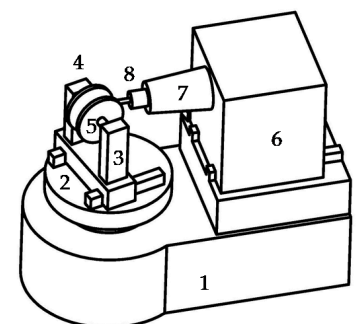
## 2. Analysis Method of Machining Error of Globoidal Cam

### 2.1. Machining Error Analysis of Globoidal Cam Profile

According to the motion law of the globoidal cam mechanism and the machining by generation method, the special machine tool for globoidal cam is designed. By using the relative motion of the tool and the workpiece to simulate the relative motion between the pre-designed globoidal cam and the driven turntable, the machining of globoidal cam is realized. The special machine tool is a four-axis double linkage structure. The overall structure of it is shown in Figure 2b. The machine tool consists of two rotary axes and two slide motion axes, which are noted by  $A$ ,  $B$  and  $W$ ,  $Z$  in order. The  $A$ -axis and the  $B$ -axis are rotation axes and they are linked with each other to realize the rotation and swing of the globoidal cam during the machining process. The  $W$ -axis and  $Z$ -axis are linear motion axes, which are used to control the feed amount of the tool and the center distance of the workpiece respectively.



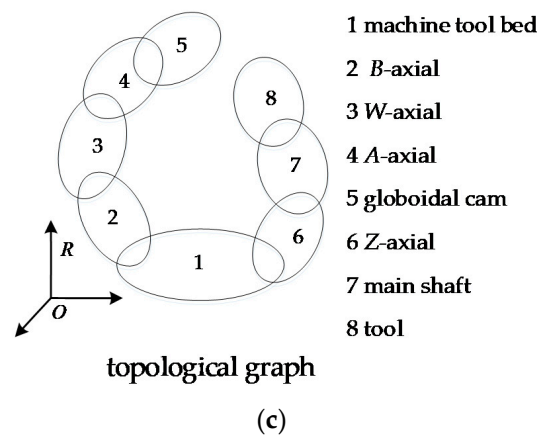
(a)



machine structure

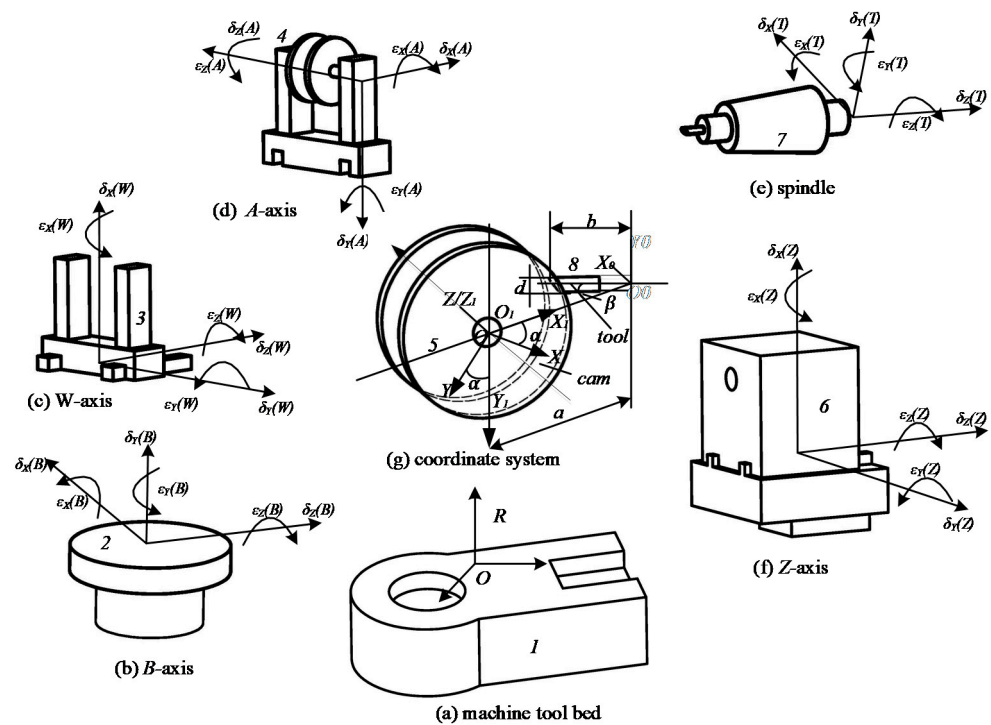
(b)

Figure 2. Cont.



**Figure 2.** Special machine tool for globoidal cam and establishment of coordinate system. (a) The special machine tool for globoidal cam; (b) Machine tool structure; (c) Machine tool kinematics.

According to the theory of multi-body system, there are two branches of machine tools: (1) tool branch; (2) workpiece branch, as shown in Figure 2c. There are three linear displacement errors and three angular displacement errors in the machine tool spindle, i.e., A-axis, B-axis, Z-axis, and W-axis respectively. Due to the relative motion relationship between the cam rotation angle and the driven turntable rotation angle, it is also necessary to consider the cam rotation angle and the driven rotation angle, the error of the rotation angle of the turntable, and the center distance error of the cam shaft and the driven shaft. To sum up, in the machining process, there are 33 errors in the special machine tool for the globoidal cam. For the convenience of understanding, the error decomposition diagram on the special machine tool for globoidal cam is shown in Figure 3. The error definition and symbol of the globoidal cam machining machine are shown in Table 1.



**Figure 3.** Topology and structure of the machine tool. (a) Machine tool bed; (b) B-axis; (c) W-axis; (d) A-axis; (e) Spindle; (f) Z-axis; (g) Coordinate system.

**Table 1.** Errors of the special machine tool.

Error Type	Linear Offset Error			Rotational Error		
	X	Y	Z	X	Y	Z
Spindle	$\delta_X(T)$	$\delta_Y(T)$	$\delta_Z(T)$	$\varepsilon_X(T)$	$\varepsilon_Y(T)$	$\varepsilon_Z(T)$
Z-axis	$\delta_X(Z)$	$\delta_Y(Z)$	$\delta_Z(Z)$	$\varepsilon_X(Z)$	$\varepsilon_Y(Z)$	$\varepsilon_Z(Z)$
B-axis	$\delta_X(B)$	$\delta_Y(B)$	$\delta_Z(B)$	$\varepsilon_X(B)$	$\varepsilon_Y(B)$	$\varepsilon_Z(B)$
W-axis	$\delta_X(W)$	$\delta_Y(W)$	$\delta_Z(W)$	$\varepsilon_X(W)$	$\varepsilon_Y(W)$	$\varepsilon_Z(W)$
A-axis	$\delta_X(A)$	$\delta_Y(A)$	$\delta_Z(A)$	$\varepsilon_X(A)$	$\varepsilon_Y(A)$	$\varepsilon_Z(A)$
Cam Angle	–	–	–	–	–	$\Delta\alpha$
Turntable Angle	–	–	–	–	–	$\Delta\beta$
Center Distance	$\Delta a$	–	–	–	–	–
Turntable	$\delta_X(S)$	$\delta_Y(S)$	$\delta_Z(S)$	$\varepsilon_X(S)$	$\varepsilon_Y(S)$	$\varepsilon_Z(S)$

## 2.2. Multibody System Characteristic Transformation Matrix

The characteristic transformation matrix of the multi-body system is represented by homogeneous coordinates. The homogeneous coordinate transformation includes six transformation methods: linear displacement along the three coordinate axes and angular displacement around the three coordinate axes. Each motion can be obtained by the principle of the homogeneous coordinate transformation. Therefore, the transformation matrix of the machine tool spindle error coordinate system, the turntable B-axis error coordinate system, the rotary A-axis error coordinate system, the power support W-axis error coordinate system, and the spindle slide Z-axis error coordinate system can be obtained. The transformation matrix includes linear displacement transformation matrix and angular displacement transformation matrix. The machine tool errors matrix is listed in Table 2.

**Table 2.** Representation method of the transformation matrix.

Coordinate System	Linear Displacement			Angular Displacement		
	X	Y	Z	X	Y	Z
Spindle	$t_{TX}$	$t_{TY}$	$t_{TZ}$	$r_{RX}$	$r_{RY}$	$r_{RZ}$
B-axis	$t_{BX}$	$t_{BY}$	$t_{BZ}$	$r_{BX}$	$r_{BY}$	$r_{BZ}$
A-axis	$t_{AX}$	$t_{AY}$	$t_{AZ}$	$r_{AX}$	$r_{AY}$	$r_{AZ}$
W-axis	$t_{WX}$	$t_{WY}$	$t_{WZ}$	$r_{WX}$	$r_{WY}$	$r_{WZ}$
Z-axis	$t_{ZX}$	$t_{ZY}$	$t_{ZZ}$	$r_{ZX}$	$r_{ZY}$	$r_{ZZ}$
Cam Angle	–	–	–	–	–	$r_\alpha$
Turntable Angle	–	–	–	–	–	$r_\beta$
Center Distance	–	–	$t_a$	–	–	–

## 2.3. Profile Modeling and Error Sensitivity Analysis of Globoidal Cam

### 2.3.1. Modeling of Globoidal Cam Profile

When deriving the globoidal indexing cam profile equation, three rectangular coordinate systems are established. The coordinate system  $O_0X_0Y_0Z_0$  is a fixed coordinate system. Its origin  $O_0$  is the intersection point between the center axis of the cutter and the swinging centerline of the workpiece, i.e., the intersection point of the center axis of the Z-axis and the B-axis. The  $O_0Z_0$  axis overlaps with the centerline of the cutter, i.e., overlapping with Z-axis. The  $O_0Y_0$  axis overlaps with the swinging centerline of the workpiece, i.e., overlapping with the centerline when B-axis moves. The coordinate system  $O_1X_1Y_1Z_1$  oscillates around the B-axis and the  $O_1Z_1$  axis overlaps with the workpiece rotation centerline, i.e., it overlaps with the centerline when A-axis moves. The  $O_1X_1$  axis overlaps with the line  $O_1O_0$ , i.e., parallel with the W-axis. The coordinate system is fixed with the workpiece. Making the coordinate system  $O_1X_1Y_1Z_1$  rotate around the  $O_1Z_1$  axis, the rotation angle is equal to the angular displacement of A-axis movement. Then, we can get the coordinate system  $OXYZ$ . The point  $P$  on the centerline of the cutter is a random point on the theoretical

profile after processing. The theoretical profile of globoidal indexing cam is generated by using point  $P$  and through the generating method.  $b$  is the distance between the point  $P$  and the point  $O_0$ ,  $d$  is the diameter of the cutter,  $a$  is the distance between the  $A$ -axis rotation center line and the  $B$ -axis swing centerline of machine tool, i.e., the distance between cam rotation center axis line and the cam swing center axis line, which is called center distance. The relation between  $\alpha$  and  $\beta$  is determined by the motion law of a pre-designed globoidal indexing cam mechanism, which is a known condition.

According to the coordinate system and the characteristic transformation matrix based on multi-body theory, the position vector  $p_0$  of the point  $p$  in the coordinate system  $O_0X_0Y_0Z_0$  is as in (1).

$$p_0 = \begin{pmatrix} x_0 \\ y_0 \\ z_0 \end{pmatrix} = (t_{BX}t_{BY}t_{BZ}r_{BX}r_{BY}r_{BZ})(t_{ZX}t_{ZY}t_{ZZ}r_{ZX}r_{ZY}r_{ZZ})(t_{TX}t_{TY}t_{TZ}r_{TX}r_{TY}r_{TZ})t_b \quad (1)$$

The position vector  $p_1$  of the point  $p$  in the coordinate system  $O_1X_1Y_1Z_1$  is as in (2).

$$p_1 = \begin{pmatrix} x_1 \\ y_1 \\ z_1 \end{pmatrix} = (t_{wx}t_{wy}t_{wz}r_{wx}r_{wy}r_{wz})r_\beta p_0 + t_a \quad (2)$$

The position vector  $p$  of the point  $p$  in the coordinate system  $OXYZ$  is as in (3).

$$p = \begin{pmatrix} x \\ y \\ z \end{pmatrix} = t_\alpha p_1 \quad (3)$$

The unit normal vector of the theoretical profile after machining is as in (4).

$$n = \frac{\frac{\partial p}{\partial b} \times \frac{\partial p}{\partial \alpha}}{\left| \frac{\partial p}{\partial b} \times \frac{\partial p}{\partial \alpha} \right|} \quad (4)$$

The actual profiles on both sides of the processing are represented by  $p_l$  and  $p_r$ , respectively, and the solution is as in (5) and (6).

$$p_l = p - \frac{d}{2}n \quad (5)$$

$$p_r = p + \frac{d}{2}n \quad (6)$$

Adding (3) and (4) to Equations (5) and (6), the error model of the globoidal indexing cam profile can be obtained.

Setting all the error values in Table 1 as 0, the theoretical profile equation of globoidal indexing cam can be obtained.

### 2.3.2. Error Sensitivity Analysis of Globoidal Cam Machining

Combined with the theoretical profile model of the globoidal cam, the machining error of the globoidal cam profile is defined as the projection of the machining error along the normal direction  $n_N$  of the ideal profile. The profile machining error can be expressed as the difference between the actual machining profile  $p_c$  and the theoretical machining profile  $p_N$ . Set the machining error values  $e_1, e_2, \dots, e_n$ , and the error vector of the globoidal cam machining machine  $E = (e_1, e_2, \dots, e_n)$ . The machining error  $f(E)$  can be expressed as in (7).

$$f(E) = (p_c - p_N) * n_N, E = (e_1, e_2, \dots, e_n) \quad (7)$$

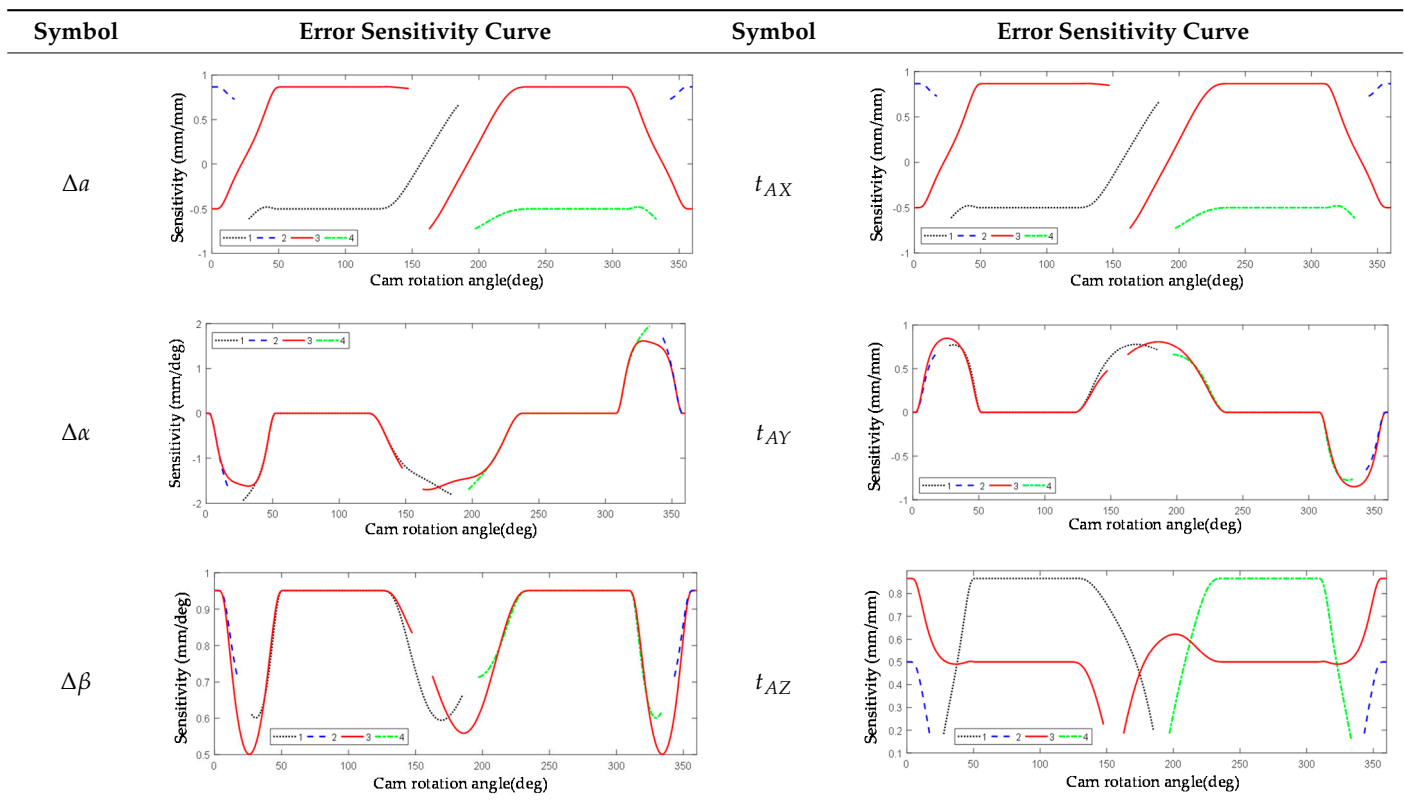
According to Taylor’s formula, the Taylor expansion formula of  $f(E)$  at  $E_0 = 0$  can be obtained as in (8), where  $f(E) = 0$ .

$$f(E) = \sum_{i=1}^n \left( \frac{\partial f}{\partial e_i} \right) e_i \tag{8}$$

where  $\partial f / \partial e_i$  is the machine tool error sensitivity coefficient, which is expressed as the influence of the machining error  $e_i$  on the machining error of the globoidal cam profile surface. Next, the effects of angular displacement error and linear displacement error on the globoidal cam profile will be discussed separately.

Through the numerical method, the error sensitivity coefficient curve of the special machining machine tool for globoidal cam is calculated by using MATLAB. Taking the center distance error, cam rotation angle error, rotation angle error, and A-axis displacement error as examples, the error sensitivity coefficient curve is as in Table 3.

Table 3. Error sensitivity curve.



It can be found that there are many errors that have no effect on the dwell segments, such as  $\delta_Y(T)$ ,  $\delta_Z(T)$ , etc. Among them,  $\delta_X(T)$ ,  $\delta_Y(T)$ ,  $\Delta\alpha$ ,  $\Delta\beta$ ,  $\Delta a$ ,  $\epsilon_X(A)$ ,  $\epsilon_Y(A)$ , and  $\epsilon_X(B)$  have the greatest influence on the error.

### 3. Evaluation and Traceability of Machining Error of Globoidal Cam

#### 3.1. Measurement Method of Machining Error of Globoidal Cam

By analyzing the characteristics of the globoidal cam profile and the function of CMM, the measurement scheme of the equidistant profile model is proposed. The four-axis measurement system is composed of CMM and the turntable.

As shown in the Figure 4, the measurement of the characteristic line of the globoidal cam equidistant profile at the specified angle can be realized, the probe radius compensation can be avoided, and the measurement speed and accuracy can be improved. In the actual

measurement, the probe is directly compared with the corresponding points on the equidistant profile model of the globoidal cam to complete the error evaluation and traceability.

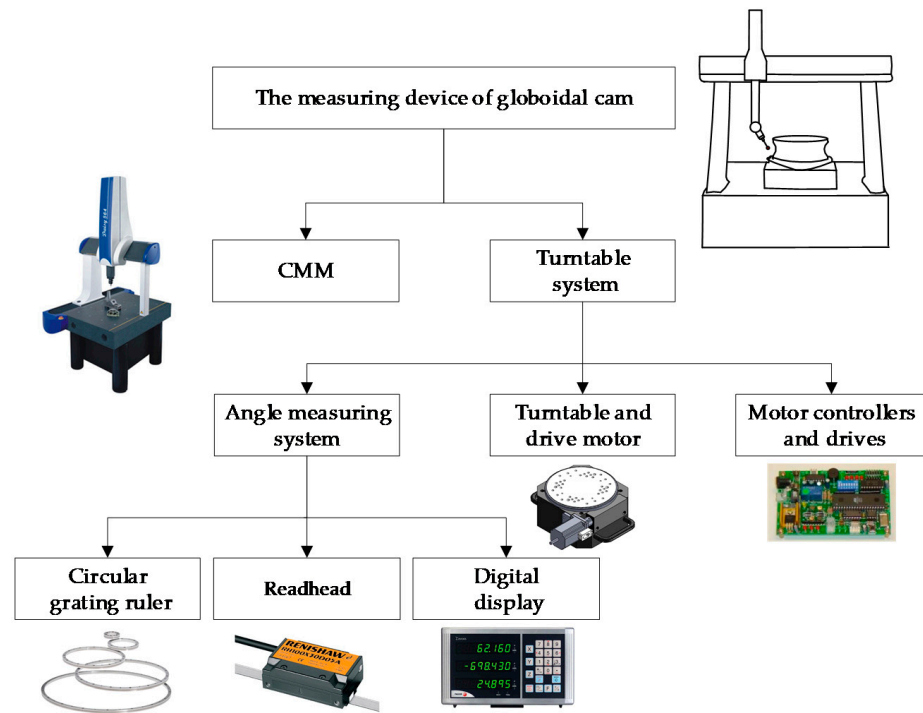


Figure 4. Structure of online measuring system for globoidal cam.

### 3.2. Evaluation of Machining Error of Globoidal Cam

The definition of the characteristic lines of the globoidal cam profile surface is given here:  $S_a$  is the axial section when the cam is transferred to  $a$ . When  $a = 0$ , the axial section  $S_0$  is the reference plane, and the reference plane remains unchanged in the process of cam rotation. The intersection line of  $S_a$  and  $S_p$  is defined as the characteristic line. The characteristic lines will be on the axial section, and the coordinate points of the working profile that meet the conditions form the axial section characteristic line. The coordinate system for solving the characteristic line of the globoidal cam profile and the axial section profile is shown in Figure 5.

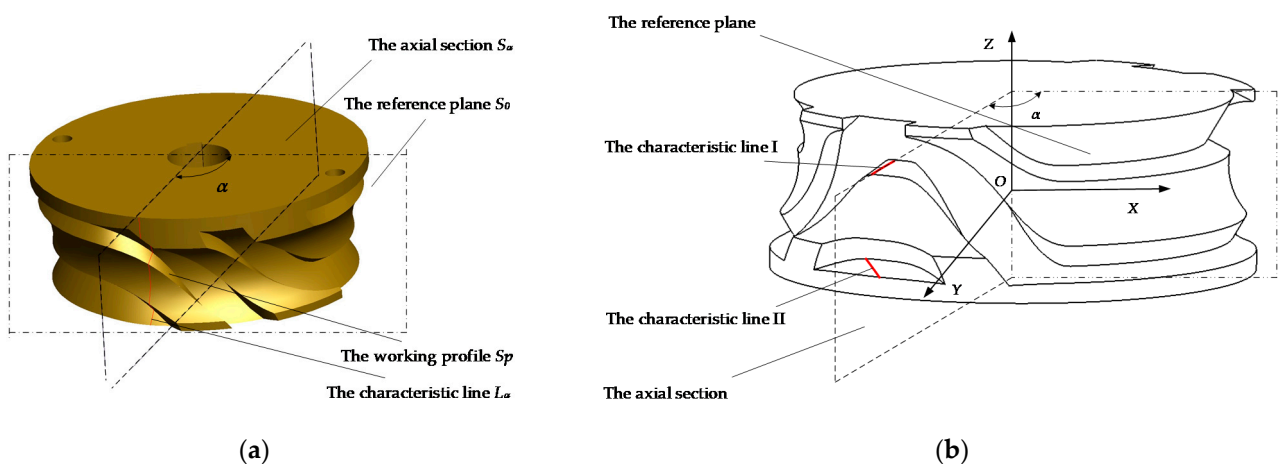


Figure 5. Globoidal cam characteristic line and coordinate system. (a) Globoidal cam profile and characteristic line; (b) Coordinate system of globoidal cam characteristic line.

The planning of the globoidal cam measurement characteristic line is as follows:

- (1) Measuring characteristic lines in the dwell segments:
  - (a)  $[358^\circ, 2^\circ]$ , four characteristic lines are planned with  $1^\circ$  as a unit;
  - (b)  $[52^\circ, 122.5^\circ]$ , 10 characteristic lines are planned with  $5^\circ$  as a unit;
  - (c)  $[237.5^\circ, 308^\circ]$ , 10 characteristic lines are planned with  $5^\circ$  as a unit.
- (2) Measuring characteristic lines in the indexing segments:
  - (a)  $[2^\circ, 52^\circ]$ , 10 characteristic lines are planned with  $5^\circ$  as a unit;
  - (b)  $[122.5^\circ, 237.5^\circ]$ , 23 characteristic lines are planned with  $5^\circ$  as a unit;
  - (c)  $[308^\circ, 358^\circ]$ , 10 characteristic lines are planned with  $5^\circ$  as a unit.

To realize error evaluation, three models are established, namely the ideal model, the actual model, and the measured model. In the process of error evaluation, it is necessary to reduce the difference between the measured model and the actual model and to find out the error between the actual model and the ideal model, and then judge whether the cam is qualified. For the error of globoidal cam, different methods are developed to evaluate the error according to different characteristics.

### 3.2.1. Error Evaluation of the Characteristic Line of the Dwell Segments

The characteristic line of the dwell segments is a straight line. Since the maximum error value of the straight line is generally at the endpoint, the two-point method is used to solve the error. The specific process is:

- (a) Fit the measurement points to a straight line as the evaluation benchmark;
- (b) Solve the coordinates of the endpoints of the theoretical characteristic line;
- (c) Find the distance from the two ends of the theoretical characteristic line to the actual characteristic line, and judge whether it is within the tolerance range.

According to the definition of the axial section and the characteristic line, the characteristic line equation can be expressed as in (9).

$$\begin{cases} z_i = k_i * \sqrt{x_i^2 + y_i^2} + b_{zi} \\ z_{i+1} = k_i * \sqrt{x_{i+1}^2 + y_{i+1}^2} + b_{zi} \end{cases} \quad (9)$$

$$k = \sum_{i=1}^n k_i, b_z = \sum_{i=1}^n b_{zi} \quad (10)$$

$$X = \sqrt{x^2 + y^2}, L = k * X + b_z \quad (11)$$

Find the distance from the two endpoints to the measured characteristic line, then the larger value is the profile error of the characteristic line at the  $\alpha$  angle, as in (12).

$$\Delta L_\alpha = \max \left\{ \frac{|kX_1 - z_1 + b_z|}{\sqrt{k^2 + 1}}, \frac{|kX_2 - z_2 + b_z|}{\sqrt{k^2 + 1}} \right\} \quad (12)$$

### 3.2.2. Evaluation of the Error of the Characteristic Line of the Indexing Segments

The characteristic line of the indexing segments is a curve, and the minimum area evaluation is used for error evaluation, as shown in Figure 6. The specific process is:

- (a) Use NURBS to fit the actual measurement points into a curve, as the error evaluation benchmark;
- (b) Solve the coordinates of the theoretical characteristic points;
- (c) Use the segmentation search method to determine the shortest distance from the theoretical characteristic point to the actual characteristic curve, and judge whether it is within the tolerance range.

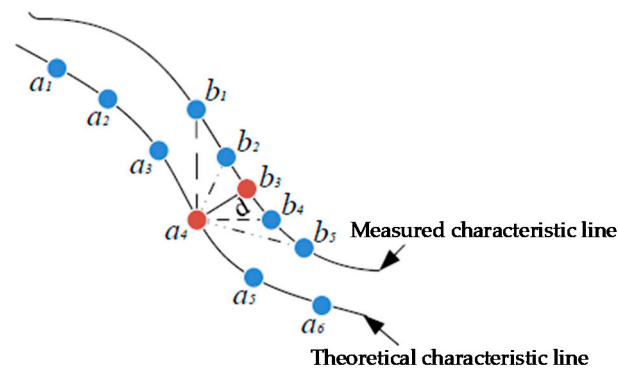


Figure 6. Minimum area assessment.

For the theoretical characteristic point  $a_4$ , there is only one point  $b_3$  located on the measured characteristic line, so that the distance between  $a_4$  and the measured characteristic line is minimized, as in (13).

$$mind = \sqrt{(a_{4x} - b_{3x})^2 + (a_{4y} - b_{3y})^2 + (a_{4z} - b_{3z})^2} \quad (13)$$

According to the definition of line profile error, the maximum distance from each theoretical characteristic point to the measured characteristic point is taken as the line profile error, as in (14).

$$\max(mind), i = 1, 2, \dots, n \quad (14)$$

### 3.2.3. Evaluation of Surface Profile Error

In this paper, the section method is used as the evaluation method of the surface profile error. The indexing segments and the dwell segments need to be evaluated for the surface profile respectively. Solve the errors of multiple globoidal cam characteristic lines separately and take the maximum value of these errors as the surface profile error.

$$\max[\Delta L_i] \quad (15)$$

After the error evaluation, it is necessary to judge whether the globoidal cam meets the accuracy requirements. If it meets the requirements, there is no need to trace the error. If it does not meet the requirements, it is necessary to trace the error to the test results.

### 3.3. Traceability of Machining Errors of Globoidal Cam

Errors are grouped according to machine tool error sensitivity. In the evaluation process of the error in the dwell segments, the errors that have no effect on the profile machining of the globoidal cam in the dwell segments can be temporarily ignored, and the source of the influential errors can be traced. The rest of the errors are traceable in the indexing segments.

The sequential quadratic programming algorithm has the advantages of fast convergence speed and high computational efficiency. In this paper, it is used as an optimization algorithm for error tracing. The optimization model needs to be established first. The general mathematical problem model of nonlinear constraints is as in (16).

$$\begin{cases} \min f(X) \\ \text{s.t. } g_u(X) \leq 0, (u = 1, 2, \dots, p) \\ h_v(X) = 0, (v = 1, 2, \dots, m) \end{cases} \quad (16)$$

$X \in R^n$ : Decision variables

$f(X)$ : Objective function

$g_u(X)$ : Inequality constraint function

$h_v(X)$ : Equality constraint function

The optimization model of processing error traceability is as follows.

- (1) Design variables: The design variables of error traceability are all errors of machine tool processing, and the method of segmental traceability is adopted.
- (2) Constraints: The constraints of this optimization model need to ensure that the calculation point is located on the globoidal cam profile. The error model of the globoidal cam profile is summarized as in (17).

$$\begin{cases} f_{ix} = f(\alpha, b, X) \\ f_{iy} = f(\alpha, b, X) \\ f_{iz} = f(\alpha, b, X) \end{cases} \quad (17)$$

where  $f_{ix}f_{iy}f_{iz}$  is the theoretical profile point coordinates  $(x, y, z)$  of the globoidal cam with error.  $\alpha$  is the cam angle,  $B$  is the tool depth, and  $X$  is the cam profile error.

$$X = (\delta_X(T), \delta_Y(T), \dots, \varepsilon_Z(S)) \quad (18)$$

- (3) Objective function: An objective function based on least squares theory is proposed, as in (19).

$$\max f(x) = \frac{1}{\sum_{i=1}^n \sqrt{(x_i - f_{ix})^2 + (y_i - f_{iy})^2 + (z_i - f_{iz})^2}} \quad (19)$$

where  $n$  is the number of measurement points.  $x_i, y_i,$  and  $z_i$  are the coordinate values of the points after alignment adjustment, which are called actual coordinate values. When using the sequential quadratic programming method to trace the source of the error, it is finally necessary to obtain a set of error values to maximize the value of the fitness function  $f(x)$ . At this time, this set of errors is the error traceability result.

#### 4. Experimental Research on Profile Error Detection for Globoidal Cam

To verify the correctness and feasibility of the machining error analysis and traceability method of the globoidal indexing cam, the accuracy of the indexing transmission was tested by the rolling experiment of the globoidal cam. If it does not meet the requirements, a *CMM* can be used to detect the machining error of the working profile of the globoidal cam, feeding back the error traceability results to the processing link, to improve the machining quality of the cam through error compensation. Thus, the integrated method of globoidal cam design, machining, and measurement is realized. This experiment was carried out in the production and processing workshop of Beiyi Machine Tool Co., Ltd. (Xiantao, China), and the experimental object is the *TC40* globoidal cam.

##### 4.1. Testing Experiment of Globoidal Cam Indexing Transmission Accuracy

The globoidal cam indexing transmission detection system is shown in Figure 7, including a rolling globoidal cam detector, a control cabinet, and an industrial computer. The transmission accuracy detection system of the globoidal cam indexing mechanism can detect the transmission accuracy of various types of globoidal cams. The rolling globoidal cam detector has five motion axes, namely  $X, Y, Z, A,$  and  $B,$  among which  $X$  and  $Y$  are manual axes,  $Z$  and  $A$  are AC motor drive axes, and the  $B$  axis is a servo motor drive axis.  $A$  and  $B$  axes are equipped with photoelectric encoders, and  $X, Y,$  and  $Z$  axes are equipped with grating rulers. The control and measurement process of the transmission accuracy detection realizes the control of each axis motor through the measurement and control software of the industrial computer and collects and displays the signals of each grating ruler and encoder.

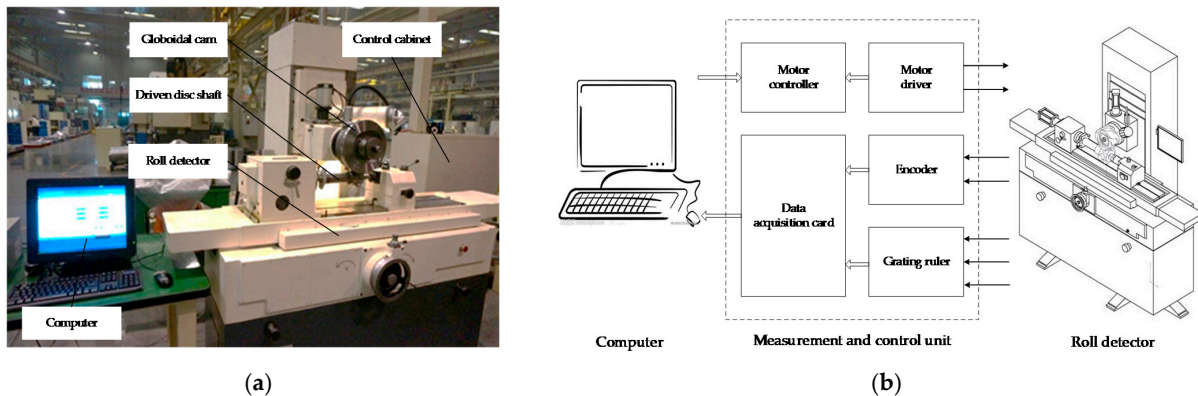


**Figure 7.** Globoidal cam Precision Inspection System. (a) Globoidal cam transmission precision detection device; (b) Schematic of precision detection system for globoidal cam.

After completing the field detection experiment, the collected data need to be analyzed and processed. The encoder data collected by the globoidal cam transmission accuracy detection system need to be phase-matched with the shaft rotation angle of the globoidal cam and the driven shaft rotation angle, then compared with the theoretical motion law curve to analyze the transmission accuracy. In this example, the modified sinusoidal motion law can be used to calculate the relationship between globoidal cam angle  $\alpha$  and the rotational angle  $\beta$  of the driven turntable at different motion positions.

Through the comparison between the globoidal cam I transmission curve and the theoretical transmission curve, as shown in Figure 8, it can be analyzed that there are obvious differences with the theoretical curve, especially in the two dwell segments, and the angular displacement of the follower is obviously small. There are many factors affecting the transmission accuracy of the globoidal cam. The globoidal cam profile error caused by machining is the main factor affecting the transmission accuracy. This requires measuring and evaluating the machining error of the globoidal cam profile and improving the machining quality after the traceability and compensation of the machining error.

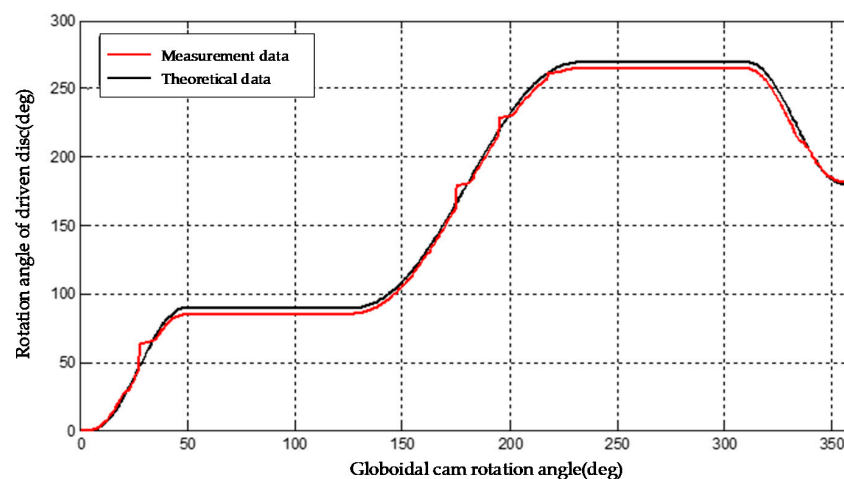


**Figure 8.** Transmission curve of CAM I.

#### 4.2. Measurement Experiment Process

The experimental device for measuring the error of the globoidal cam profile is shown in Figure 9. The device mainly consists of a three-coordinate measuring machine, a turntable system, and a globoidal cam to be measured. The model of the CMM is NHC-Y564, and the measuring stroke is as follows: X-axis-500 mm, Y-axis-600 mm, Z-axis-400 mm. The turntable system includes a turntable, positioning module, circular grating angle measurement system, driving stepper motor, turntable controller, and driver. The turntable

is controlled by a stepping motor, a single-chip microcomputer is used as the main control chip of the stepping motor control system, and the rotation angle of the turntable is displayed in real time through a circular grating angle measurement system. It can meet the measurement requirements of TC40 and TC50 series of globoidal cams. The model of globoidal cam to be tested is TC40, and its size parameter is as follows: thickness 97 mm, maximum diameter 265 mm.

Measure the characteristic points on the characteristic line of the specific cam angle position after the theoretical model matches the angle position of the cam to be measured. After all characteristic points are measured, adjust the turntable to the next position to be measured through the turntable control panel, read the angle displayed by the digital display, rotate and match the theoretical model, and complete the measurement of the next characteristic line. Repeat the above process until all characteristic lines are measured. According to the measurement plan of the characteristic line, the globoidal cam is measured in sections according to the above measurement process. After the measurement is completed, the measurement results are exported. The error evaluation and traceability at different periods are carried out according to the actual measurement data.

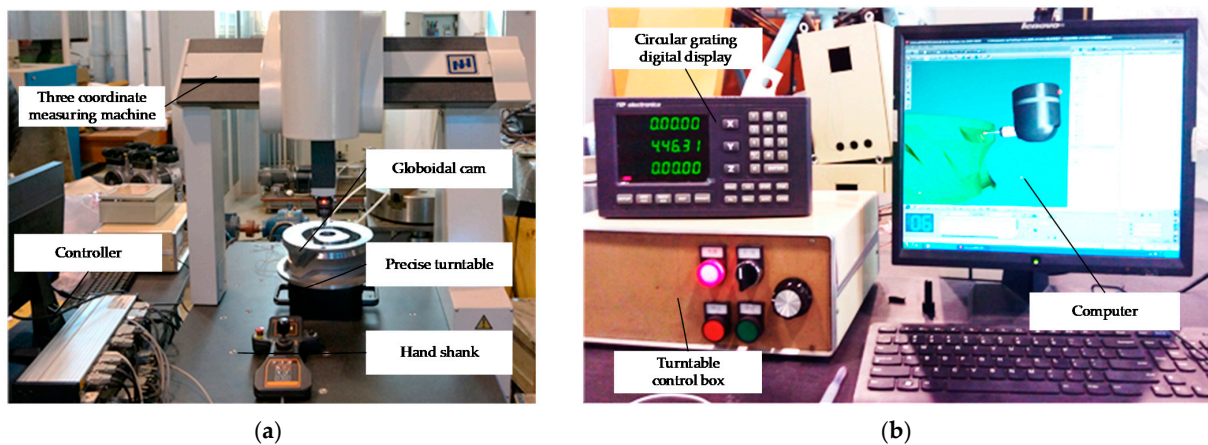


Figure 9. Equipment of measurement system control. (a) Equipment of measurement system control I; (b) Equipment of measurement system control II.

The measurement result of CMM is composed of two parts: the coordinate value of the theoretical characteristic point and the coordinate value of the measured characteristic point. The data format of results is  $PT(X, Y, Z)$ . By exporting a file in PDF format, the measuring position of the probe is displayed as shown in Figure 10a and the measuring data are shown in Figure 10b.

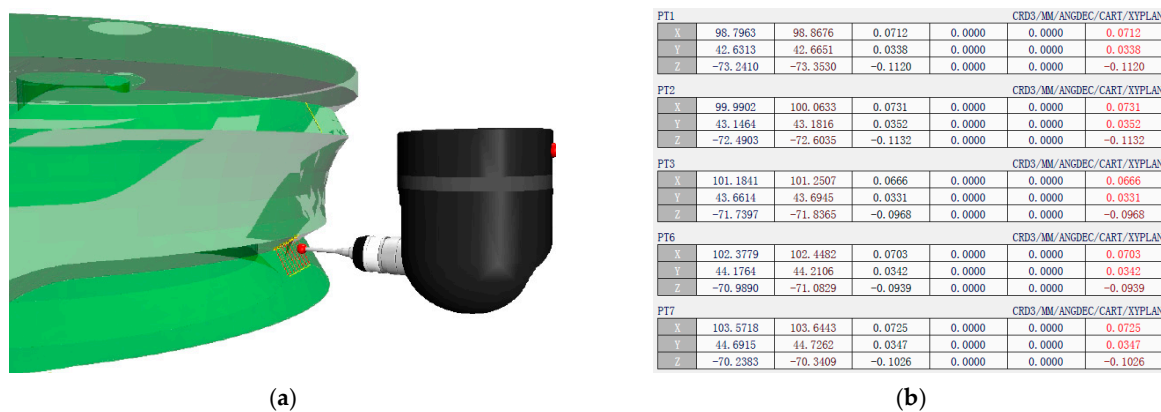


Figure 10. Results of CMM. (a) Measuring position; (b) Measuring data.

### 4.3. Error Evaluation for Globoidal Cam

#### 4.3.1. Evaluation of the Error of the Characteristic Line of the Indexing Segment

In the period of indexing segment 1, the cam angle range is  $[2^\circ, 52^\circ]$ , and 10 characteristic lines are planned at  $5^\circ$  intervals. In the actual measurement, it is not necessary to precisely control the rotation angle of the turntable. When the turntable stops, record the relative angle measured by the circular grating relative to the reference axis section, and calculate the theoretical characteristic line according to the cam rotation angle to match the measured data to complete the error evaluation. In the period of indexing segment 1, taking the third characteristic line  $L_{e3}$  (cam rotation angle  $\alpha = 15.15^\circ$ ) as an example, the evaluation process of the contour error of the indexing segment line is introduced in detail. The measurement data of the characteristic points are shown in Table 4.

**Table 4.** The error evaluation result of the indexing segment 1.

Cam Angle Position ( $^\circ$ )	Upper Profile Error (mm)	Lower Profile Error (mm)
5.1250	0.1550	0.0350
10.5125	0.1574	0.0345
15.1500	0.1456	0.0330
20.0510	0.1389	0.0294
25.0650	0.1439	0.0288
30.4510	0.1530	0.0279
35.1230	0.1463	0.0253
40.1380	0.1553	0.0251
45.0690	0.1491	0.0299
50.1250	0.1550	0.0289

#### 4.3.2. Evaluation of the Characteristic Line Error of the Dwell Segment

According to the result of the characteristic line measurement plan, the cam rotation angle interval at the dwell segment 2 is  $[52^\circ, 122.5^\circ]$ . In order to evaluate the profile error of the dwell segment line of the globoidal cam, taking the third characteristic line  $L_3$  as an example, the detection is completed according to the detection process. The theoretical and measured points of the cambered cam are summarized as shown in Table 5.

**Table 5.** The evaluation result of the contour error of the rest Section 2.

Cam Angle Position ( $^\circ$ )	Upper Profile Error (mm)	Lower Profile Error (mm)
60.1250	0.1845	0.0155
65.5250	0.1745	0.0155
70.0125	0.1833	0.0149
75.1125	0.1689	0.0138
80.9425	0.1762	0.0165
85.2145	0.1699	0.0165
90.3468	0.1762	0.0170
95.6712	0.1789	0.0168
100.4536	0.1880	0.0160
105.6921	0.1723	0.0159

In this paper, the measurement method of the equidistant profile axis section characteristic line adopted is consistent with the section method in the surface profile error evaluation method, so the section method is adopted as the evaluation method of the globoidal cam surface profile error. The indexing segment and the dwell segment need to be evaluated for the surface profile respectively.

The detected globoidal cam profile error is within the tolerance range of the profile error determined, and it is rated as a qualified product, which is consistent with the detection result of the plug gauge in the production workshop, indicating the correctness of the assessment method.

#### 4.4. Error Traceability for Globoidal Cam

Due to the large number of processing error factors, this paper selects 8 errors to trace the source of the error, which are as follows:

- (1) Linear displacement error of the main shaft along X direction  $\delta_X(T)$
- (2) Linear displacement error of the main shaft along Y direction  $\delta_Y(T)$
- (3) Center distance error  $\Delta a$
- (4) Cam angle error  $\Delta\alpha$
- (5) Follower angle error  $\Delta\beta$
- (6) Angular displacement error of A axis around X direction  $\varepsilon_X(A)$
- (7) Angular displacement error of A axis around Y direction  $\varepsilon_Y(A)$
- (8) B axis angular displacement error around X direction  $\varepsilon_X(B)$

According to the method of segmental traceability of machining errors proposed in this paper, the error factors affecting the dwell are found in the dwell segments, and the other errors are found in the indexing segment. By solving various processing error sensitivity coefficients, the displacement error of the spindle along the Y direction  $\delta_Y(T)$ , the angular displacement error of the A axis around the X direction  $\varepsilon_X(A)$ , the angular displacement error of the B axis around the X direction  $\varepsilon_X(B)$ , and the cam angle error  $\Delta\alpha$  have no effect in the dwell segment.

First, in the dwell segment, according to the measurement characteristic line, the line displacement error of the spindle along the X direction  $\delta_X(T)$ , the center distance error  $\Delta a$ , the follower angle error  $\Delta\beta$ , and the angular displacement error of the A axis around the Y direction  $\varepsilon_Y(A)$  are traced to the source. Then, trace the source of the remaining four errors by using the measuring characteristic line of the indexing segment. The traceability results are shown in Table 6.

**Table 6.** Summary of actual error value and traceability value.

Machining Error	Error Parameter	Traceability Results
$\delta_X(T)$	<i>Delta_x</i>	0.0050 mm
$\Delta a$	<i>Delta_a</i>	0.0120 mm
$\Delta\beta$	<i>Delta_beta</i>	0.0056 rad
$\varepsilon_Y(A)$	<i>Delta_Gamma_y</i>	0.0023 rad
$\delta_Y(T)$	<i>Delta_y</i>	0.0035 mm
$\Delta\alpha$	<i>Delta_Alpha</i>	0.0069 rad
$\varepsilon_X(A)$	<i>Delta_Gamma_x</i>	0.0068 rad
$\varepsilon_X(B)$	<i>Delta_delta_x</i>	0.0119 rad

#### 4.5. Testing Experiment of Transmission Accuracy

According to the result of error tracing, adjust the program of the globoidal cam machining machine, carry out error compensation, and test the transmission accuracy of the globoidal cam after compensation. The transmission curve of the globoidal cam II is shown in Figure 11, which is basically consistent with the ideal cam, and the machining quality is significantly improved compared with the globoidal cam I, which shows that the proposed method for analyzing the machining error and tracing the source of the globoidal indexing cam is feasible.

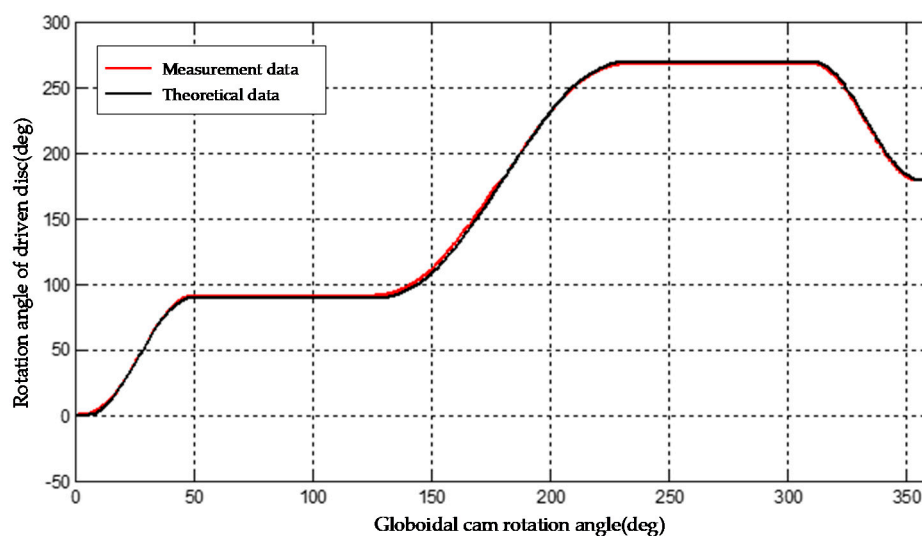


Figure 11. The transmission curve of CAM II.

## 5. Discussion

The globoidal cam indexing mechanism is mainly composed of globoidal cams, turntables, boxes, camshafts, turntable shafts, bearings, and other components. The output accuracy of the globoidal cam indexing mechanism is related to the manufacture of each component and the assembly of each component. The error sources of the globoidal cam indexing mechanism are mainly the machining geometric errors of its components, as well as the assembly errors of the globoidal cam and the turntable, the camshaft, the turntable shaft, and the box. These errors have an impact on the output motion accuracy of the globoidal cam indexing mechanism.

The machining error of the globoidal cam indexing mechanism is a major factor that affects the indexing accuracy of the globoidal cam indexing mechanism, and it is also a difficult factor to analyze. In this paper, the assembly of the indexing mechanism box is not carried out, and only the machining error of the globoidal cam profile and the center distance error are analyzed. The correlation between the machining error of the globoidal cam and the transmission precision of the globoidal cam indexing mechanism, as well as the influence of the center distance adjustment on the transmission precision, are found. This provides a theoretical basis for designing the precision distribution, processing technology adjustment, and formulating the precision index system of the special processing machine tool for globoidal cams.

## 6. Conclusions

Based on the multi-body system theory, this paper establishes the profile error model of the globoidal cam and evaluates and traces the error. The proposed method is applied to the machining of the globoidal cam in the factory, which improves the machining quality and provides a key technology for the integration of the design, manufacture, and measurement of the globoidal cam. The main conclusions can be summarized as follows:

- (1) Based on the multi-body system theory, the special machine tool for globoidal cam machining is analyzed, and the error transfer matrix of globoidal cam machining is deduced. The machining error model of the globoidal cam is established, and a method for comprehensively analyzing the machine tool through the curve of the error sensitivity coefficient of the globoidal cam is proposed. Through the method, the influence law of each error on the globoidal cam profile can be obtained.
- (2) By analyzing the characteristics of the globoidal cam profile, a method of segmental measurement and error evaluation of the globoidal cam profile characteristic line and grouping traceability of machining errors is proposed. The dwell segments adopt the two-point method, and the index segments adopt the minimum area method.

- According to the analysis results of the error sensitivity of the globoidal cam profile, the sequential quadratic programming method is used to trace the processing errors, which improves the data processing speed and the accuracy of the traceability results.
- (3) By building a measurement system for globoidal cam transmission accuracy and profile error, the method proposed in this paper is used to evaluate and trace the error of the measurement results, and the machining error compensation of the machine tool is carried out according to the results of error traceability. The experimental results show that the error evaluation and traceability method proposed in this paper can improve the machining accuracy of the globoidal cam.

**Author Contributions:** Methodology, S.S. and Y.Q.; software, Y.Q. and Z.G.; validation, Y.Q., Z.G. and C.H.; writing—original draft preparation, Y.Q., Z.G. and C.H.; writing—review and editing, S.S.; project administration, S.S.; funding acquisition, S.S. All authors have read and agreed to the published version of the manuscript.

**Funding:** This research was funded by the National Science and Technology Major Project, China, grant number 2013ZX04008-021, and in part by the Beijing Excellent Young Engineer Innovation Studio Project, under grant number S2001013202101.

**Institutional Review Board Statement:** Not applicable.

**Informed Consent Statement:** Not applicable.

**Data Availability Statement:** Not applicable.

**Acknowledgments:** The authors would like to acknowledge the support and contribution from the Beijing Beiyi Machine Tool Co., Ltd. (Beijing, China) for their help with manufacturing and be grateful to the Key Lab of Mechanical Engineering, Beijing University of Technology, China.

**Conflicts of Interest:** The authors declare no conflict of interest.

## References

- Ge, Z.H.; Bie, Y.; Jiao, D.; Zhang, T.Y. Study on the profile modification of globoidal indexing cams. *Mech. Trans.* **2014**, *38*, 160–162.
- Yu, J.W.; Huang, K.F.; Luo, H. Manipulate optimal high-order motion parameters to construct high-speed cam curve with optimized dynamic performance. *Appl. Math. Comput.* **2020**, *371*, 1–13. [[CrossRef](#)]
- Li, Y.L.; Gou, W.D.; Li, J.Y.; Zhou, X.L. Research on the comprehensive performance test specification of chain knife library and manipulator. *Mach. Hyd.* **2017**, *45*, 154–159.
- Shi, D.F.; Cao, J.J.; Liang, J.S. Design of offset type redundant globoidal cam. *Mech. Trans.* **2017**, *41*, 187–190.
- Calleja, A.; Fernandez, A.; Rodriguez, A.; De Lacalle, L.N.L.; Lamikiz, A. Turn-milling of blades in turning centres and multitasking machines controlling tool tilt angle. *J. Eng. Manuf.* **2014**, *229 Pt B*, 1–13. [[CrossRef](#)]
- Xia, T.; Xu, L.; Si, J.X. The study of globoidal indexing cam CNC machine tools. *Adv. Mat. Res.* **2013**, *753–755*, 888–891. [[CrossRef](#)]
- Chen, H.; Zhang, Y.M.; Bu, F.H. Parametric design of globoidal indexing CAM. *Mach. Des. Manuf.* **2007**, *6*, 3.
- Cheng, H.Y. Optimum tolerance for globoidal cam mechanisms. *JSME. Int. J. Ser. C* **2002**, *45*, 519–526. [[CrossRef](#)]
- Yang, S.; Wen, Z.; Li, L. Research on tolerance allocation of globoidal cam mechanism based on improved optimal limit deviation method. *Chin. Mech. Eng.* **2014**, *25*, 731–736.
- Yin, M.F.; Lyu, C.Y.; Zhao, Z.H. The theoretical study of CAM processing theory and the calculation method of the influence of CAM body deviation error on the profile error are studied. *J. Shandong Univer. Technol.* **2001**, *15*, 18–21.
- Ji, S.T.; Zhang, Y.M.; Zhao, J. The influence of center distance error of machining center of globoidal cam on convex contour error. *J. Beijing Univ. Technol.* **2014**, *40*, 825–830.
- Zhang, Y.M.; Ji, S.T.; Zhao, J. Tolerance analysis and allocation of special machine tool for manufacturing globoidal cams. *Adv. Manuf. Technol.* **2016**, *87*, 1597–1607. [[CrossRef](#)]
- Bu, F.H.; Zhang, Y.M.; Shang, D.G. Study on machining error of globoidal cam profile resulting from rotational deviation of location of part in machining. *Adv. Mat. Res.* **2012**, *452–453*, 211–218.
- Wang, X.F.; Tang, L. Measurement theory and implement of globoidal indexing cam using CMM. *J. Tianjin Univ.* **2011**, *44*, 1024–1028.
- Lin, P.D.; Hsieh, J.F. Dimension inspection of spatial cams by CNC coordinate measuring machines. *J. Manuf. Sci. Eng.* **2000**, *122*, 149–157. [[CrossRef](#)]
- Liang, Y.D.; Song, L.J. Three-dimensional modeling of globoidal indexing cam. *Mach. Design Manuf.* **2006**, *8*, 2.
- Lin, X.J.; Wang, Z.Q.; Shan, C.W. Method of probe radius compensation for free surface measurement by CMM. *Aeronaut. Manuf. Technol.* **2011**, *10*, 75–78.

18. Wu, P.L.; Hu, D.F. Tool path optimization of globoidal cam flank milling based on spatial linear-regression analysis. *J. Adv. Mech. Des. Syst. Manuf.* **2019**, *13*, 60. [[CrossRef](#)]
19. Wu, P.L.; Hu, D.F. Error control of non-equal diameter machining of globoidal cam profile based on adaptive method. *J. Braz. Soc. Mech. Sci.* **2020**, *42*, 160–162. [[CrossRef](#)]
20. Abderazek, H.; Yildiz, A.R.; Mirjalili, S. Comparison of recent optimization algorithms for design optimization of a cam-follower mechanism. *Int. J. Knowl.-Based Syst.* **2019**, *11*, 1–52. [[CrossRef](#)]
21. Nguyen, T.T.N.; Kurtenbach, S.; Hüsing, M. A general framework for motion design of the follower in cam mechanisms by using non-uniform rational B-spline. *Mech. Mach. Theory* **2019**, *137*, 374–385. [[CrossRef](#)]
22. Sateesh, N. Improvement in motion characteristics of cam follower systems using NURBS. *Des. Manuf. Technol.* **2014**, *8*, 15–21. [[CrossRef](#)]
23. Xia, B.Z.; Liu, X.C.; Shang, X. Improving cam profile design optimization based on classical splines and dynamic model. *J. Cent. South Univer.* **2017**, *24*, 1817–1825. [[CrossRef](#)]
24. Sun, S.W.; Jiang, Z.Q.; Huang, J.; Yang, J.W. Analysis and Detection Method for Machining Error of Globoidal Indexing Cam Profile. In Proceedings of the Asia Conference on Mechanical and Materials Engineering: ACMME, Seoul, Korea, 15–18 June 2018; p. 213.